Results in Physics 15 (2019) 102749

Contents lists available at ScienceDirect

Results in Physics

journal homepage: www.elsevier.com/locate/rinp

# Quantum model for the effect of thiols adsorption on resistivity of gold ultrathin films

Ricardo Henríquez*, Claudio Gonzalez-Fuentes, Valeria del Campo, Jonathan Correa-Puerta, Carolina Parra, Francisca Marín, Patricio Häberle

*Departamento de Física, Universidad Técnica Federico Santa María, Av. España 1680, Valparaiso 2390123, Chile*

ARTICLE INFO

*Keywords:*
Electrical resistivity
Fractal description
Thiols
Ultra thin films
Coating

ABSTRACT

The predominant role of surface scattering, in electronic transport through nanoscale thin films, was examined by measuring and modeling the change in resistivity induced by the adsorption of thiols on the surface. For this purpose, gold ultrathin films on sapphire, using chromium as surfactant, were prepared through thermal evaporation, seeking to maximize the surface induced dispersion. A maximum resistivity increase of 13.5% was observed, in an 8 nm Au/Cr/Sapphire sample. This is the highest reported value for such films to date. The morphology of the samples was measured by STM and characterized through height-difference correlation function. A fractal self-affine representation of the surface was found, and it was modified to account the thiol effect: the scattering center due to the adsorption of a molecule was modeled as a void in the surface. This change was related to the electrical transport of the film through two quantum models: the Palasantzas and Barnas (PB) theory and the Sheng, Xing and Wang theory, extended by Munoz et al. (mSXW). For our samples, the mSXW theory did not predict a resistivity change, while the PB theory provides a good description of the experimental resistivity increase due to thiols adsorption as function of thickness.

## Introduction

The trend towards miniaturization of electronic circuits has driven the size of the structures conducting electrical current down to ~10 nm [1]. However, at room temperature, most metals used for this purpose (Cu, Au, Ag) present a mean free path of about 40 nm. Therefore, the understanding of the mechanisms that generates the resistance in such structures and its relationship with "size effects" is a relevant issue for further development of current device technologies [2–5].

At room temperature, there are three main mechanisms which control the resistivity of a metallic ultrathin film: electron phonon scattering, electron grain boundary scattering and electron-surface scattering. Therefore, the main experimental challenge of a series of recent reports, has been to separate the contribution of each one of them, in order to understand their individual effect in nanoscale conducting channels [6–9]. In a recent work by our group [6], the *method of thiol adsorption* in Au films, was presented as a mean of identifying the surface scattering contribution in such structures. This method consists in tuning changes in the fabrication conditions of the samples, seeking the highest effect on the resistivity due to the adsorption of a thiol self-assembled monolayer (SAM). The film with the highest resistivity increase allows the identification of the fabrication conditions in which electron-surface scattering is the most relevant [6]. Two critical conditions in the sample fabrication procedure were identified in that report: the use of a chromium layer between the gold film and the substrate (as metallic surfactant), and the substrate temperature during evaporation ($T_S$ ~ 360 K).

Once the effect of electron-surface scattering is identified as a relevant contribution to resistivity, different electrical transport theories can be used to understand the effects of surface phenomena on the film conductivity. Whereas semi-classical theories have been used to explain the changes in resistivity due to thiols adsorption [10–12], the application of models based on quantum theories has not been sufficiently explored (a discussion about different quantum theories on electrical transport in metallic thin films can be found in Refs. [2;13]). In those theories the morphological characteristics of the films have been used to describe relevant transport properties, using the self-correlation function or the height-correlation function of the surface as inputs for the calculations. On the other hand, it has been experimentally demonstrated that one of the best descriptions of the surface, can be achieved by means of a self-affine representation [14–17], in which the self-correlation function or the height-correlation function can be

* Corresponding author.
*E-mail address:* ricardo.henriquez@usm.cl (R. Henríquez).

https://doi.org/10.1016/j.rinp.2019.102749
Received 19 July 2019; Received in revised form 10 October 2019; Accepted 13 October 2019
Available online 21 October 2019

adjusted through a self-affine function [14,18,19].

In this work, gold ultrathin films on sapphire were evaporated introducing a chromium layer as metallic surfactant. Then, using the *method of thiol adsorption,* the substrate temperature that maximizes the electron-surface scattering was determined. Samples fabricated under these conditions were used to study the effect of thiols adsorption on the film resistivity through a model based on electrical transport quantum theories and the self-affine description of the surface.

## Experimental and theoretical background

### *Thiols adsorption and semi-classical transport theory*

From the point of view of how the resistivity of a thin film is changed, the adsorption of thiols corresponds to an interface/surface process. That is, the molecular adsorption affects mainly the electron-surface scattering. Essentially, most of the thiols bind with their S-head into the gold surface, creating new scattering centers at the surface [6,10–12,20,21]. The consequential resistivity change can then be computed by the following expression:

$$\frac{\Delta\rho}{\rho} = \frac{\rho_{with\ thiols} - \rho_{without\ thiols}}{\rho_{without\ thiols}}$$

where $\rho_{with\ thiols}$ is the film resistivity when thiol molecules cover almost the entire sample's surface, and $\rho_{without\ thiols}$, corresponds to the film resistivity with a "clean" (uncoated) surface.

Although a previous report has stated that the effect of molecule adsorption on the electric transport is thickness-independent [10], when plotting the resistivity change reported by different authors for different molecular lengths and film thicknesses, the size effect becomes evident as is depicted in Fig. 1.

Fig. 1 shows that the highest resistivity increase, upon molecular adsorption, depends on film thickness (full symbols). The change in the film's resistivity is a reflection of a different sensitivity to electron-surface scattering each particular film thickness. It is important to highlight that Zhang et al. [21] have demonstrated experimentally that the alkyl chain length does not affect the resistivity change of the film, therefore, the phenomenon is independent of the molecule used for the study (in Fig. 1, C10, C12, or C16).

From a theoretical approach, the standard theory of size effects is the most employed theory to model film's resistivity changes and it is known as the Fuchs-Sondheimer theory (FS theory) [22,23]. Briefly, the motion of electrons in the film is modeled through a Boltzmann transport equation, which considers, in the sample interfaces (upper and lower surfaces), a specularity parameter "*P*" that represents the fraction of electrons specularly scattered by the interface. This theory was extended by Lucas [24], enabling two different specularity parameters for each interface (film-air and film-substrate): "*P*" and "*Q*". Finally, Namba [25] also considered the thickness profile of the sample through a trigonometric function $t(x) = \bar{t} + t'sin(kx)$, where "$\bar{t}$" is the mean thickness, "$t'$" is the amplitude of the oscillation, and "$k$" describes the spatial periodicity of the oscillation. The final expression to compute film's resistivity changes is:

$$\frac{\rho}{\rho_0}(\bar{t}, t', \ell_0, P, Q) = \frac{\bar{t}}{L}\int_0^L \frac{\frac{\rho}{\rho_{0FS}}\left(\frac{t(x)}{\ell_0}, P, Q\right)}{t(x)}dx \quad (1)$$

where

$$\frac{\rho}{\rho_{0\,FS}}(\kappa, P, Q) = \frac{\varphi_{P,Q}(\kappa)}{\kappa}$$

$$\frac{1}{\varphi_{P,Q}(\kappa)} = \frac{1}{\kappa} - \frac{3}{4\kappa^2}\int_1^\infty \left(\frac{1}{x^3} - \frac{1}{x^5}\right) \frac{(1 - e^{-\kappa x})[2 - P - Q + (P + Q - 2PQ)e^{-\kappa x}]}{1 - PQe^{-2\kappa x}}dx$$

$\kappa = \bar{t}/\ell_0$,

"$\ell_0$" is the bulk mean free path (mean free path in the absence of surface scattering), and "$\rho_0$" the bulk resistivity (resistivity in the absence of surface scattering).

Finally, the effect of the thiols on the resistivity can be calculated from:

$$\frac{\Delta\rho}{\rho} = \frac{\rho_{with\ Thiols} - \rho_{without\ Thiols}}{\rho_{without\ Thiols}} = \frac{\frac{\rho}{\rho_0}(\bar{t}, t', \ell_0, P_T, Q) - \frac{\rho}{\rho_0}(\bar{t}, t', \ell_0, P_C, Q)}{\frac{\rho}{\rho_0}(\bar{t}, t', \ell_0, P_C, Q)} \quad (2)$$

where "$P_C$" represents the specularity parameter of the gold surface without thiols (clean), and "$P_T$", the specularity parameter of the film surface covered by thiols.

In Fig. 1, the continuous line represents the thickness dependence given by the semi-classical theoretical prediction, computed through Eq. (2) with $Q = 0.2$, $P_C = 0.4$, $P_T = 0.2$, $t' = 4.5$ nm, $\ell_0 = 38$ nm and $\rho_0 = 22.4$ nΩ·m (the first four values following Ref. [12], and the last two values correspond to gold bulk at RT [26]).

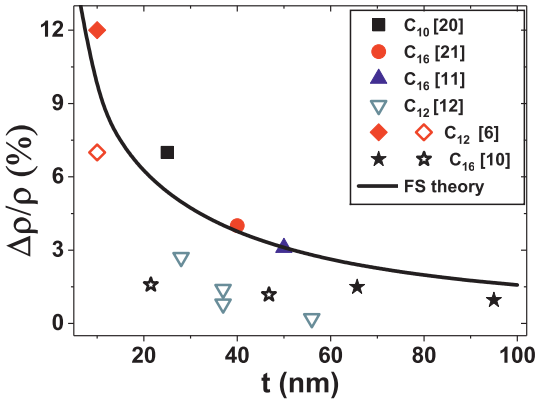


**Fig. 1.** Resistivity change Δρ/ρ due to thiols adsorption on gold thin films as a function of sample thickness. Different symbols are used to represent different references: square symbols depict $C_{10}$ [20]; round symbols, $C_{16}$ [21]; triangles, $C_{16}$ [11]; stars, $C_{16}$ [10]; inverted triangles, $C_{12}$ [12]; diamonds, $C_{12}$ [6]. Full symbols were used to highlight samples that show the most significant effect. Continuous line represents the prediction of FS theory for $Q = 0.2$, $P_C = 0.4$, $P_T = 0.2$, and $t' = 4.5$ nm.

### *Quantum transport theories*

As stated in the introduction section, many theories have studied the effect of electron-surface scattering on electrical transport through quantum models [2,13], however only two of them have based their descriptions of the surface on a self-affine representation.

In 1997, Palasantzas and Barnas [27] published a theory (PB theory) based on a description of Fishman and Calecki [28] of electrical transport in a thin film. Briefly, in this model the thin film is considered as an ideal quasi-bidimensional structure, in which two parts compose the Hamiltonian that describe the system. The first, is associated to a free-particle motion, parallel to the film's plane. The other, is determined by a unidimensional potential that confines electrons in a direction perpendicular to the film's surface. This second part defines sub-bands in the dispersion law. A Boltzmann Transport Equation governs the Fermi Dirac distribution function of the electrons for each sub-band, adding inter-bands transitions through the collision-term. The roughness of the film's upper surface is defined through a random function $h(\mathbf{r})$, where $\mathbf{r}$ is the in-plane position vector. This function modifies the film thickness, and therefore, the Hamiltonian that

describes the system. In PB theory, $h(r)$ is depicted by a self-affine representation.

In 1995, Sheng et al. [29] published a different model for the electron-surface scattering in a thin film. Briefly, instead of using a Boltzmann Transport Equation, this theory is based on determining the Green function for the Hamiltonian described above plus a term to account impurity-electron scattering. Then, using the Kubo formula, the conductivity in the real space is calculated. In 2002, Munoz et al. [30], extended this theory to a model in which the surface is represented by a self-affine function (mSXW theory).

## Materials and methods

### *Sample fabrication*

Gold (99.999% purity, Alfa Aesar) and chromium (99.994% purity, MaTeck) were deposited through thermal evaporation from tungsten baskets in a high vacuum system (turbomolecular pump and diaphragm pump; P ~ $1 \times 10^{-4}$ Pa or lower during the evaporation). The substrate was sapphire (C-axis, LED grade, Alfa Aesar), previously annealed during 24 h at 1100 °C, for surface improvement (that is, to diminish surface defects) in accordance with the process described by Kästle et al. [31]. The film thickness and evaporation rate were measured with quartz microbalances (QM). The thickness obtained by this method was previously calibrated with values obtained from ellipsometry (custom made ellipsometer) and atomic force microscopy (AFM, Omicron VT SPM) measurements. The sample holder was made of copper and it included an oven and a thermocouple to measure and assist the control of the substrate ($T_S$) and annealing ($T_A$) temperatures. Also, a mask, placed on top of the substrate, enabled the evaporation of the film with a four-contacts shape. All contacts were fixed on one side of the film, to avoid their immersion into the thiol solution.

The film fabrication was separated in six steps (all performed in the vacuum system). First, the sapphire substrate was annealed at ~120 °C, for two hours. Next, the oven was switched off, and the substrate was held in this condition until the next day. Second, a chromium 0.8 nm thick layer was deposited at room temperature (rate = 1.2 nm/min). Third, sample temperature was slowly increased during approximately three hours to achieve the desired $T_S$. Fourth, the gold film was evaporated with a rate of 0.8 nm/min. Fifth, the sample was annealed after gold evaporation by keeping the film at $T_S$ another hour after ending deposition. Sixth, the oven was switched off, and the sample was taken out of the vacuum system after ~15 h, for thiol's deposition process.

Self-assembled monolayers, SAMs, were prepared by immersing the ultrathin film into a freshly prepared 1 mM solution of dodecanethiol ($C_{12}H_{25}SH$, 98% purity, Aldrich) in absolute ethanol (p.a. grade, Aldrich). More details about fabrication and characterization of the SAMs can be found in Refs. [6] and [12].

### *Electrical characterization*

The electrical characterization was performed through the resistance measurement using the four-contacts method. A current of ~10 μA and 310 Hz fed the sample, and voltage signals were acquired through computer controlled lock-in amplifiers (SR830, Stanford Research).

The resistance was measured before samples were immersed in the solution, and during the thiols adsorption process. The standard deviation of the resistance before thiols adsorption was always lower than 0.02%. The resistivity change due to thiols adsorption was determined from the resistance measured 25 min after immersion of the sample [6].

### *Morphological characterization*

Sample surface was characterized through Scanning Tunneling Microscopy (STM, Omicron VT SPM) in Ultra High Vacuum at room temperature, before and after thiols deposition. The tips were made from Pt/Ir wire, and checked by imaging HOPG surface with atomic resolution.

A complete description of the surface can be obtained studying the height-difference correlation function "$g$" and its dependency on the scale of distances "$R$" [32]. This function, $g(R)$, can be calculated from the expression:

$$g(R) = g(|\boldsymbol{r} - \boldsymbol{r}'|) = \frac{1}{S}\int_S^{\hat{A}\cdot} (h(\boldsymbol{r}) - h(\boldsymbol{r}'))^2 d\boldsymbol{r}' \tag{3}$$

where $h(r)$ is the height in the point $\boldsymbol{r}$, and $S$ denotes the sampled surface. From STM images, $g(R)$ was obtained (eight to ten images for sample). The optimum size of the images to study the behavior of $g(R)$ was $250 \times 250\ \text{nm}^2$ with a resolution of $512 \times 512$ pixels.

In 1993, Palasantzas et al. [18] proposed three functions to represent $g(R)$ when the surface of metallic films is modeled as a self-affine surface. Among them, the most used representation is:

$$g(R) = 2\delta^2\left(1 - exp\left[\left(-\frac{R}{\xi}\right)^{2H}\right]\right) \tag{4}$$

where δ, ξ and $H$ are known as surface roughness, lateral correlation length and roughness exponent, respectively.

## Results and analysis

In order to enhance the electron-surface scattering, Au/Cr/Sapphire 10 nm thick films were evaporated at different temperatures: 360, 415 and 460 K. Next, thiol adsorption process was performed, and the resistivity increment was measured. Fig. 2a shows the resistivity increase due to thiols adsorption as a function of substrate temperature ($T_S$) for these Au/Cr/Sapphire samples (round symbols). Resistivity changes for Au/Cr/Mica 10 nm thick samples reported in a previous work [6] are also displayed (square symbols). Table 1 shows $t$ (film thickness), $T_S$ and Δρ/ρ for these Au/Cr/Sapphire samples, which are labeled as S1, S2 and S5.

Results show that the Au/Cr/Sapphire sample fabricated at ~415 K displays the largest resistivity change due to thiols adsorption. This temperature is higher than that found for Au/Cr/Mica samples (~360 K). This difference reveals a different contribution from electron upper surface scattering to electrical conduction, due to use of sapphire instead of mica as substrate.

Keeping $T_S$ at 410 K, the effect of film's thicknesses, $t$, on the resistivity change due to thiols adsorption was studied. Three samples, with $t$ = 8, 10 and 12 nm, were prepared and labeled as S4, S5 and S6 (Table 1). Fig. 2b depicts the resistivity increase as a function of thickness for these three samples. Results show that by reducing films thicknesses, the resistivity change due to thiols adsorption increases from 7.3% to 13.6%. This increment in resistivity change, as film

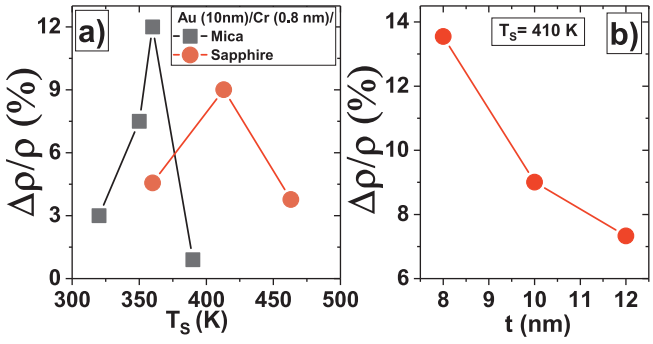


**Fig. 2.** a) Substrate temperature dependence of resistivity increase due to thiols adsorption on Au/Cr/Sapphire (round symbols) and on Au/Cr/Mica samples (square symbols) [6]. b) Thickness dependence of resistivity increase due to thiols adsorption for Au/Cr/Sapphire samples.

**Table 1**
Fabrication conditions of the samples: thickness, $t$; substrate temperature, $T_S$; and resistivity increase due to thiols adsorption, $\Delta\rho/\rho$. Morphological parameters obtained from self-affine adjustment: surface roughness, δ; lateral correlation length, ξ; and roughness exponent, $H$.

| | $t$ (nm) | $T_S$ (K) | $\Delta\rho/\rho$ (%) | δ (nm) | ξ (nm) | $H$ |
|---|---|---|---|---|---|---|
| S1 | 10 | 360 | 4.5 | 1.8 | 16 | 0.85 |
| S2 | 10 | 463 | 4.0 | 4.5 | 37 | 0.83 |
| S3 | 10 + 4 | 415 | 0.6 | 2.2 | 20 | 0.75 |
| S4 | 8 | 415 | 13.6 | 3.4 | 27 | 0.88 |
| S5 | 10 | 415 | 9.01 | 3.7 | 19 | 0.83 |
| S6 | 12 | 415 | 7.33 | 3.4 | 28 | 0.83 |

thickness decreases, is indeed an expected behavior, since electron-surface scattering becomes a more relevant dispersion mechanism compared to other bulk related processes. The size effect is then manifestly evident for this thickness range. Additionally, the change of 13.6% is the highest resistivity change value reported for this phenomenon in gold thin films (see Fig. 1).

To study the relationship between film's surface morphology and its electrical response, the height-difference correlation function $g(R)$ and its scale length dependence were determined. Fig. 3a shows $g(R)$ for samples S3 y S4. Fig. 3b and c display representative STM images of these two samples. The continuous lines in Fig. 3a represent the adjustment through the self-affine function (Eq. (4)). Table 1 shows the parameters obtained from the self-affine adjustment of all samples.

In all samples, the self-affine function showed a good representation of $g(R)$ (similar to samples S3 and S4 in Fig. 3a), independent of $t$ and $T_S$. Previous works experimentally confirmed the hypothesis which states that the gold surface could be considered as fractal self-affine. This was demonstrated for different fabrication conditions in samples evaporated on mica [14,15] and on glass [16,17]. From our results, this hypothesis can be extended to ultrathin films fabricated on a surfactant layer.

The adjustment parameters of the traces in Fig. 3 are expected to represent morphological characteristics of the sample surface: δ is related to root mean square (rms) roughness amplitude; ξ, to the mean grain size; and $H$, to "the degree of surface irregularity" [27]. From Table 1, comparing the parameters of samples S1, S2 and S5, all with the same thickness, it is evident that a rise in $T_S$ generates an increase in the grain size and in the rms roughness amplitude. This change in the morphology is similar to other previously reported in the same temperature range [6] for gold thin films on mica. Compared to these changes, the variation in thickness from 8 to 12 nm (S4, S5 and S6), produces only slight differences in δ and ξ parameters. On the other hand, the roughness exponent value, $H$, is between 0.83 and 0.88, except for S3. These values are similar to those reported for gold on mica ($0.82 < H < 0.87$) [14]. Sample S3 was fabricated in a different way. In a first step, 10 nm layer was deposited and 2 min later, a new 4 nm layer was added on top. In this film, the representation of g(R) through a self-affine function is as good as in the other samples, but the adjustment rendered a lower value for $H$.

In samples S4, S5 and S6, the fabrication conditions enabled the optimization of electron-surface scattering contribution to resistivity. In these samples a relationship between the parameters of the self-affine adjustment and the electrical transport coefficients is expected. In contrast, to explain the drop of sensitivity to surface scattering found in samples S1, S2 and S3, based on surface morphology is not a simple or direct task. For example, if grain boundaries exhibit high roughness, the contribution of electron grain boundary scattering to resistivity will increase, independent of the mean grain diameter [2]. In the same direction, the existence of not columnar grains [33] or the presence of defects in its crystalline structure will produce a rise in film resistance which would not correlate with the parameters describing the surface.

The next task is to apply transport electrical theories based on electron-surface scattering to explain the resistivity increase due to thiols adsorption in the samples in which the contribution of electron-surface scattering is the highest: S4, S5 and S6.

As discussed in Section "*Thiols adsorption and semi-classical transport theory*", the FS theory explains the resistivity increase based on a reduction of the specular parameter associated to the upper film surface. To study the prediction of this model, seven parameters must be determined: $Q$, $P_C$, $P_T$, $t$, $t'$, $\ell_0$ and $\rho_0$. For our samples, $\ell_0 = 38$ nm and $\rho_0 = 22.4$ nΩ·m correspond to gold bulk values at room temperature; $t$ is the film thickness; and $t'$, the surface roughness (the value reported in the fifth column of Table 1). Following the analysis presented in Section "*Thiols adsorption and semi-classical transport theory*", $Q = 0.2$, $P_C = 0.4$ and $P_T$ were used as an adjustment parameter obtained by fitting the resistivity increase of each sample. Results of this process are shown in Table 2. Similar values of $P_T$ were found for samples S5 and S6 and a slightly lower value for S4 (the thinnest sample). To compare these values with others previously reported, the reduction in the specularity parameter due to thiols adsorption must be calculated. In Table 2, $P_T$ changes with respect to $P_C$ are shown, indicating a diminution between 45% and 68%, as film thickness increases. These changes are larger

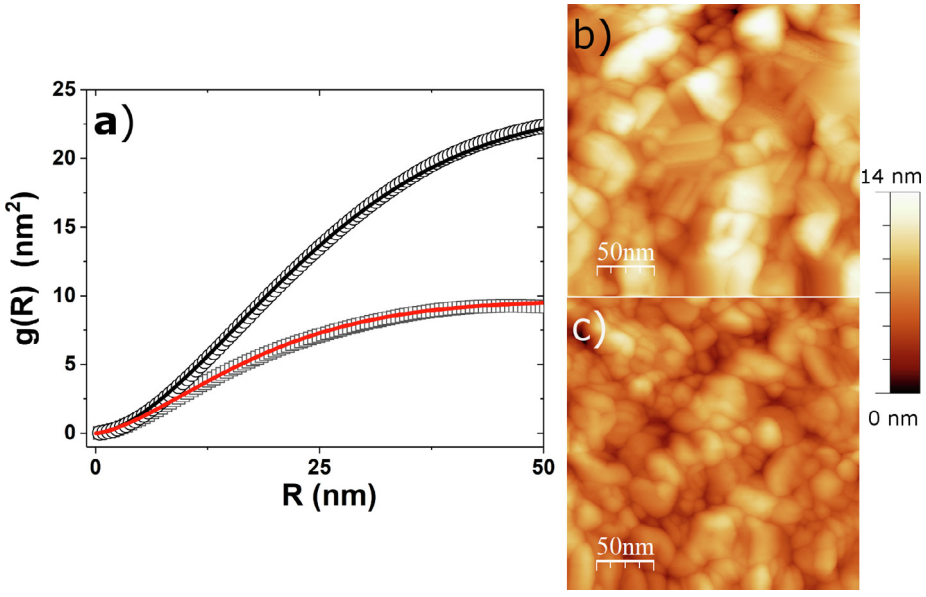


**Fig. 3.** a) Scale length dependence of the height-difference correlation function for two samples: S4 (top trace) and S3 (lower trace). Symbols depict data and the continuous lines correspond to the adjustment performed through self-affine functions. Representative STM images (size 250 × 250 nm²) of samples S4 and S3 are shown in panels b) and c). Both images were adjusted to the same color scale bar.

**Table 2**
Samples' thickness ($t$) and other parameters obtained from FS and PB theories. $P_T$: specularity parameter of the film surface covered by thiols; $(Pc - P_T)/Pc$: change in the specularity parameter due to thiols adsorption; $h$: void-depth parameter.

| Sample | t (nm) | $P_T$ | $(Pc - P_T)/Pc$ | h (nm) |
|---|---|---|---|---|
| S4 | 8 | 0.13 | 0.68 | 1.1 |
| S5 | 10 | 0.20 | 0.50 | 0.89 |
| S6 | 12 | 0.22 | 0.45 | 0.88 |

than those previously reported for samples with thicknesses between 30 and 40 nm (between 4% and 11%) [11,12]. The difference between these values highlights the existence of a size effect regarding this phenomenon.

To model the creation of a new scattering center due to the adsorption of a thiol, a modification in the surface roughness was carried out. It was implemented by removing from the film, a certain volume of material around the position where the S-head of the thiols is located. To calculate the effect of this process on $g(R)$, the height matrices z(x,y) of the STM images, were used to define the model surface. It was generated by replacing the matrix element z(x,y) by z(x,y) – $h$, in a random (x,y) position (this parameter $h$ is labeled as the "void-depth"). This process was repeated for $N$ random positions in all STM images. Fig. 4a shows a representation of one of the modified images, performed through Mathematica software.

Considering that the proposed process modifies one pixel at a time, the number $N$ of pixels can be associated to the modified area of the surface, or directly, to the thiols coverage: θ. For each sample (i.e., for each set of images), a new function $g_N(R)$ was obtained, and a new self-affine function was adjusted and associated to a covered area. Fig. 4b–d show the typical behavior of δ, ξ and H, as function of θ, respectively.

In all samples, the behavior represented in Fig. 4b–d, is the same: as θ rises, δ increases, and ξ and H decrease; and the largest change occurs in the $H$ parameter. On the other hand, the changes of the triplet (δ, ξ, $H$) are more noticeable as $h$ grows (fit not shown). The next task is to determinate how the variation of these parameters affects the theoretical prediction of the resistivity increase.

As previously mentioned, PB [27] and mSXW [29,30] theories relate the parameters of a self-affine adjustment with the film's electrical conductivity. Since $H$ is the parameter that presents the largest percentage change, the first task was to study the dependence of the

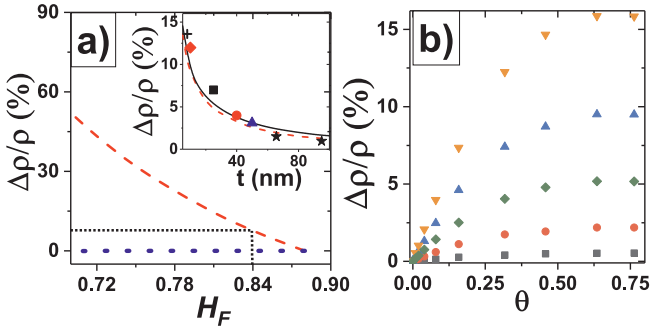


**Fig. 5.** a) Resistivity increase Δρ/ρ as a function of $H_F$ for PB [27] (dashed line) and mSXW [29,30] (dotted line) theories. Inset: Resistivity increase Δρ/ρ as function of thickness for $H_F = 0.84$. Continuous line is the FS theoretical prediction as in Fig. 1. Symbols represent the highest values of Fig. 1, except the cross that labels the value measured from sample S4. b) Resistivity increase Δρ/ρ as a function of θ as predicted by the PB theory [27]. Different symbols label values of $h$: squares, 0.25 nm; circles, 0.5 nm; diamonds, 0.75 nm; triangles, 1 nm; and inverted triangles 1.25 nm.

resistivity increase on this parameter. Starting from triplet (δ, ξ, $H$) = (3.4, 27.0, 0.88), obtained for S4, PB [27] and mSXW [29,30] theories were applied to calculate the resistivity increase:

$$\frac{\Delta\rho}{\rho}(H_F) = \frac{\rho(3.4,\ 27.0,\ H_F) - \rho(3.4,\ 27.0,\ 0.88)}{\rho(3.4,\ 27.0,\ 0.88)}$$

where $H_F$ labels the final value of $H$.

Fig. 5a shows the resistivity increase as function of $H_F$, obtained from both theories. The dashed line represents the prediction of the PB theory, whereas the dotted line denotes the one obtained from the mSXW theory. Both theories display a fundamentally different behavior: while mSXW theory predicts a slight increase lower than 0.1% as $H_F$ grows (dotted line), PB theory shows a high decrease in the same range (dashed line). On the other hand, the resistivity increase calculated by PB theory, when $H$ is modified from 0.88 to 0.84 (expected variation according to Fig. 4d), turns out to be close to 10%. This value is very close to 13%, the experimentally determined value.

The discrepancy presented by the prediction based in the mSXW theory can be explained by its formulation. This theory is based on the fact that the main contribution of electron-surface scattering to resistivity is achieved when the surface roughness reaches the scale of the

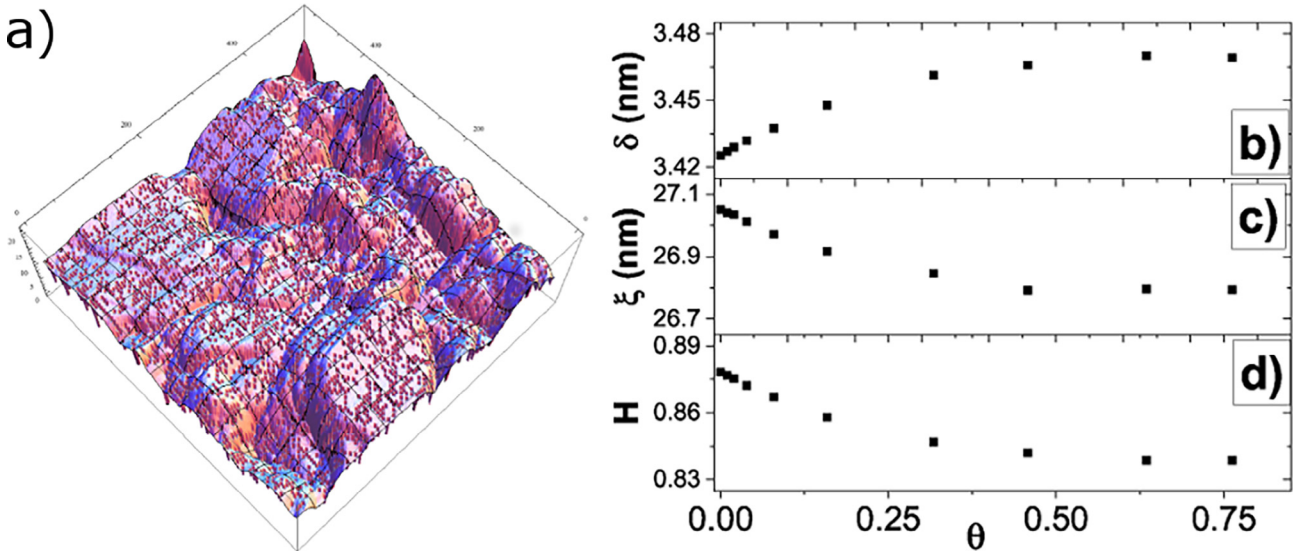


**Fig. 4.** a) Representation of the model for thiols adsorption on the film surface. Typical coverage dependence of the parameters b) δ, c) ξ and d) $H$, obtained from the self-affine representation of the surface.

Fermi wavelength [13]. In gold this value is ~0.5 nm, therefore, in samples where δ ~ 3 nm (our films), this theory has only a very minor influence, regardless of the values for ξ and *H*. Then, the model based on the mSXW theory is not applicable to our samples. Due to this evidence, henceforth, the model studied will be that based on the PB theory.

Inset of Fig. 5 shows the fractional resistivity change as a function of film thickness together with a comparison between PB (dashed line) and FS theories (continuous line). It is worth to highlight the good agreement between experimental data and predictions, even though an adjustment throughout the range was not performed (the change in *H* from 0.88 to 0.84 was used for the model based on the PB theory).

Finally, the effect of *h* on the theoretical prediction for the resistivity increase was examined. Fig. 5b shows how the resistivity increase changes as covered area (θ) rises, for different values of *h*. This plot uses the parameters determined for S4, however the behavior is similar for S5 and S6. As *h* increases, the effect is higher on Δρ/ρ, showing a saturation value for θ ~ 0.63. This is an expected result, since triplet (δ, ξ, *H*) does not show major changes for θ > 0.63. Based on this result, the value of *h* for θ ~ 0.63 was determined as a parameter that can be adjusted to obtain the resistivity increase for each sample. The last column of Table 2 shows the values obtained for *h* through this process.

Results show that the value of *h* is practically the same for S5 and S6, whereas it increases for S4. From FS theory, a similar conclusion can be obtained regarding the variations of the specularity parameters (fourth column of Table 2). This can be understood based on the existence of other contribution to the phenomenon (not included in either theories), which involved size effect. In this sense, aspects such as the modification of the band structures due to thiols adsorption needs to be considered. Different spectroscopy techniques and simulations have been used to measure the band structure of the thiol-gold system [34,35]. In the frame of the PB theory, due to the confinement, ~40 sub-bands are generated in a gold film 10 nm thick [28]. The modifications induced on them by the adsorption of thiols could have a non-negligible effect on electrical transport.

On the other hand, our model predicts a value for *h* ~ 1 nm. It is larger than that expected from analyzing Thomas-Fermi screening [36] of a sulfur atom in gold. A way to improve the model, would be to include changes in the electronic density and self-consistent potentials near the surface induced by the adsorption of the S-head of the thiol molecules.

Regarding coverage, the model shows a nonlinear relation between resistivity change and coverage, which reaches a saturation value for θ ~ 0.63. In this direction, in 2003, Tobin [37] measured simultaneously the resistance change due to S adsorption and the coverage raise, during $H_2S$ dosing of a copper 50 nm thick film. Results showed a "highly nonlinear" relation between ρ and θ, in which, the resistivity reached its saturation value before coverage did. To understand this behavior the electronic density of states of S on Cu(1 0 0) was analyzed and discussed. However, a satisfactory response was not found, stating that the sulfur coverage dependence of copper film resistivity is "a challenge to our understanding". Our model indicates that the change induced on the height difference correlation function by removing a piece of the surface diminishes as coverage increases, thus the effect of the adsorption of the first thiols is much less than that generated by the last ones. This behavior produces the nonlinear relation between ρ and θ.

On the other hand, regarding electron-surface scattering, Zheng et al. [38] deposited Ni atoms on a copper 9 nm thick film, observing a resistance increase between 14 and 19%. This change was explained through the FS theory, relating the Ni adsorption to a reduction in the specularity parameter. In our work, a similar resistance change, of ~14%, was found for the 8 nm thick sample. These results suggest that the limit for the resistance increase due electron surface scattering (for one interface) in a ~10 nm thick film is between 15 and 20%. It is clear that this value can be explained through a specularity parameter change, however the relation between this increment and the film surface roughness is not completely understood. Many works (Refs. [2;13], for example) have found correlations between these two "measurements" based on the information provided by the surface's height correlation function, however, those reports do not consider the roughness exponent *H*, starting from a gaussian correlation function. In this sense, our work clearly establishes the importance of this parameter, and it should be not ignored in future studies about this topic.

Our model could be improved through considerations as band structures or dielectric function, however it is not a simple task, because they should be also incorporated into an electrical transport theory. To the best of our knowledge, such improved model has not been developed so far. However, the promising results presented in this work, show that this type of model can be extended to other interface phenomena that affect electrical transport, such as oxidation or coating by different materials among others.

## Summary

The predominance of electron-surface scattering in thin films was analyzed through the resistivity change due to thiols adsorption, named *method of thiol adsorption*. For this purpose, gold ultrathin films on sapphire, using chromium as surfactant, were prepared through thermal evaporation. For 10 nm thick gold films (with 0.8 nm chromium layer), the electron-surface scattering effect is maximized when substrate temperature is held at 415 K during evaporation. This temperature is 55 K higher than that previously reported for Au/Cr/mica samples. Under these conditions, 8, 10 and 12 nm thick samples were fabricated. The Au/Cr/Sapphire film of 8 nm showed a resistivity increase of 13.5% due to thiol adsorption, the largest observed for gold samples to the best of our knowledge.

The morphology of the samples was measured by STM and characterized through height-difference correlation function. A fractal self-affine representation of the surface was found, and therefore, *g(R)* was adjusted through a self-affine function, which depends on three parameters: surface roughness (δ), lateral correlation length (ξ), and roughness exponent (*H*).

By modeling the scattering center due to the adsorption of a thiol as a void in the surface, a new self-affine function was obtained, and the new triplet (δ, ξ, *H*) was determined. The changes in the parameters were related to the electrical transport of the film through two quantum models: the Palasantzas and Barnas (PB) theory and the Sheng, Xing and Wang theory, extended by Munoz et al. (mSXW). For our samples, the mSXW theory didn't predict a resistivity change, whereas the PB theory provides a good description of the experimental resistivity increase due to thiols adsorption as a function of film thickness.

## CRediT authorship contribution statement

**Ricardo Henríquez:** Writing - original draft, Conceptualization, Investigation, Formal analysis, Funding acquisition, Supervision, Validation, Project administration. **Claudio Gonzalez-Fuentes:** Writing - review & editing, Conceptualization, Investigation, Formal analysis, Methodology, Software. **Valeria del Campo:** Writing - original draft, Funding acquisition, Resources, Supervision, Validation. **Jonathan Correa-Puerta:** Writing - review & editing, Investigation, Methodology. **Carolina Parra:** Writing - review & editing, Formal analysis, Methodology. **Francisca Marín:** Formal analysis, Investigation, Methodology. **Patricio Häberle:** Writing - original draft, Funding acquisition, Resources, Supervision, Validation.

## Declaration of Competing Interest

The authors declare that they have no known competing financial interests or personal relationships that could have appeared to influence the work reported in this paper.

## Acknowledgements

RH recognizes Professor Luis Moraga Jaramillo (now deceased) for his enlightening discussions on the subjects related to this article. This work was partially funded by project “Fondecyt de Iniciación 11140787” and “Fondecyt 1181905”. P. H. and V. del C. acknowledge support from “Fondecyt 1171584”.

## Appendix A. Supplementary data

Supplementary data to this article can be found online at https://doi.org/10.1016/j.rinp.2019.102749.

## References

[1] www.itrs2.net.
[2] Munoz Raul C, Arenas Claudio. Appl Phys Rev 2017;4:0111102.
[3] Zhou Tianji, Gall Daniel. Resistivity scaling due to electron surface scattering in thin metal layers. Phys Rev B 2018;97:165406.
[4] Miao Tingting, Li Dawei, Shi Shaoyi, Ji Zhongli, Ma Weigang, Zhang Xing, et al. Essential role of enhanced surface electron– phonon interactions on the electrical transport of suspended polycrystalline gold nanofilms. RSC Adv 2018;8:20679–85.
[5] Henriquez Ricardo, Bravo Sergio, Roco Roberto, del Campo Valeria, Moraga Luis, Kroeger Daniel, et al. Electrical percolation and aging of gold films. Metall Mat Trans A 2019;50:493–503.
[6] Henriquez Ricardo, Del Campo Valeria, Gonzalez-Fuentes Claudio, Correa-Puerta Jonathan, Moraga Luis, Flores Marcos, et al. The effect of electron-surface scattering and thiol adsorption on the electrical resistivity of gold ultrathin films. Appl Surf Sci 2017;407:322–7.
[7] Lucas MSP. Surface scattering of conduction electrons in gold films. Appl Phys Lett 1964;4:73.
[8] Marom H, Eizenberg M. The effect of surface roughness on the resistivity increase in nanometric dimensions. J Appl Phys 2006;99:123705.
[9] Henriquez Ricardo, Moraga Luis, Kremer German, Flores Marcos, Espinosa Andres, Munoz Raul C. Size effects in thin gold films: discrimination between electron-surface and electron-grain boundary scattering by measuring the Hall effect at 4K. Appl Phys Lett 2013;102:051608.
[10] Fried GA, Zhang Y, Bohn PW. Effect of molecular adsorption at the liquid–metal interface on electronic conductivity: the role of surface morphology. Thin Solid Films 2001;401:171.
[11] Zhang Yumo, Terrill Roger H, Bohn Paul W. Chemisorption and chemical reaction effects on the resistivity of ultrathin gold films at the liquid-solid interface. Anal Chem 1999;71:119–25.
[12] Correa-Puerta Jonathan, Del Campo Valeria, Henríquez Ricardo, Häberle Patricio. Resistivity of thiol-modified gold thin films. Thin Solid Films 2014;570:150–4.
[13] Robles Marcelo E, Gonzalez-Fuentes Claudio A, Henriquez Ricardo, Kremer German, Moraga Luis, Oyarzun Simón, et al. Resistivity of thin gold films on mica induced by electron–surface scattering: application of quantitative scanning tunneling microscopy. Appl Surf Sci 2012;258:3393–404.
[14] Munoz Raul C, Gonzalez-Fuentes Claudio A, Henriquez Ricardo, Espinosa Andres, Kremer German, Moraga Luis, et al. Resistivity of thin gold films on mica induced by electron-surface scattering from a self-affine fractal surface. J Appl Phys 2011;110:023710.
[15] Liu Zhi Hui, Brown Norman MD, McKinley Archibald. Evaluation of the growth behaviour of gold film surfaces evaporation-deposited on mica under different conditions. J Phys: Condens Matter 1997;9:59–71.
[16] Salvarezza RC, Vazquez L, Herrasti P, Ocon P, Vara JM, Arvia AJ. Self-affine fractal vapour-deposited gold surfaces characterization by scanning tunnelling microscopy. Europhys Lett 1992;20:727.
[17] Vazquez L, Salvarezza RC, Herrasti P, Ocon P, Vara JM, Arvia AJ. Scale-dependent roughening kinetics in vapor deposited gold. Surf Sci 1996;345:17.
[18] Palasantzas G, Krim J. Effect of the form of the height-height correlation function on diffuse x-ray scattering from a self-affine surface. Phys Rev B 1993;48:2873.
[19] Zhang Shangyu, Pei Yanbo, Liu Linhua. Dielectric function of polycrystalline gold films: effects of grain boundary and temperature. J Appl Phys 2018;124:165301.
[20] Pugmire DL, Tarlov MJ, van Zee RD. Structure of 1,4 benzenedimethanethiol self-assembled monolayers on gold grown by solution and vapor techniques. Langmuir 2003;19:3720.
[21] Zhang Yumo, Terrill Roger H, Bohn Paul W. In-plane resistivity of ultrathin gold films: a high sensitivity, molecularly differentiated probe of mercaptan chemisorption at the liquid-metal interface. J Am Chem Soc 1998;120:9969–70.
[22] Fuchs K. The conductivity of thin metallic films according to the electron theory of metals. Math Proc Camb 1938;34:100.
[23] Sondheimer EH. The influence of a transverse magnetic field on the conductivity of thin metallic films. Phys Rev 1950;80:401.
[24] Lucas MSP. Electrical conductivity of thin metallic films with unlike surfaces. J Appl Phys 1965;36:1632.
[25] Namba Y. Resistivity and temperature coefficient of thin metal films with rough surface. Jpn J Appl Phys 1970;9:1326.
[26] Matula RA. Electrical resistivity of copper, gold, palladium, and silver. J Phys Chem Ref Data 1979;8:1147.
[27] Palasantzas G, Barnas J. Surface-roughness fractality effects in electrical conductivity of single metallic and semiconducting films. Phys Rev B 1997;56:7726.
[28] Fishman Guy, Calecki Daniel. Surface-induced resistivity of ultrathin metallic films: a limit law. Phys Rev Lett 1989;62:1302.
[29] Sheng L, Xing DY, Wang ZD. Transport theory in metallic films: crossover from the classical to the quantum regime. Phys Rev B 1995;51:7325.
[30] Munoz Raul C, Finger Ricardo, Arenas Claudio, Kremer German, Moraga Luis. Surface-induced resistivity of thin metallic films bounded by a rough fractal surface. Phys Rev B 2002;66:205401.
[31] Kästle G, Boyen H-G, Schröder A, Plettl A, Ziemann P. Phys Rev B 2004;70:165414.
[32] Barabasi L, Stanley H. Fractal concepts in surface growth. Cambridge University Press; 1995.
[33] Moraga Luis, Arenas Claudio, Henriquez Ricardo, Bravo Sergio, Solis Basilio. The electrical conductivity of polycrystalline metallic films. Phys B 2016;499:17–23.
[34] Watkins NJ, Zangmeister CD, Chan CK, Zhao W, Ciszek JW, Tour JM, et al. Electron spectra of a self-assembled monolayer on gold: inverse photoemission and two-photon photoemission spectroscopy. Chem Phys Lett 2007;446:359–64.
[35] Correa-Puerta Jonathan, del Campo Valeria, Henríquez Ricardo, Esaulov Vladimir A, Hamoudi Hicham, Flores Marcos, et al. Unoccupied interface and molecular states in thiol and dithiol monolayers. Langmuir 2017;33:12056–64.
[36] Ashcroft Neil W, David Mermin N. Solid state physics. Thomson Learning, Inc; 1976.
[37] Tobim RG. Intralayer interaction effects on surface resistivity: sulfur and oxygen on Cu(100). Surf Sci 2003;524:183–90.
[38] Zheng PY, Deng RP, Gall D. Ni doping on cu surfaces: reduced copper resistivity. Appl Phys Lett 2014;105:131603.